Spectrochimica Acta Part B 83–84 (2013) 37–49

Contents lists available at SciVerse ScienceDirect

Spectrochimica Acta Part B

journal homepage: www.elsevier.com/locate/sab

Fused glass sample preparation for quantitative laser-induced breakdown spectroscopy of geologic materials

Patrick Pease *

Department of Geography, University of Northern Iowa, 205 Innovative Teaching & Technology Center, Cedar Falls, IA 50614 USA

ARTICLE INFO

Article history:
Received 3 December 2012
Accepted 16 March 2013
Available online 26 March 2013

Keywords:
LIBS
Calibration
Sample preparation
Major element
Mineralogy

ABSTRACT

Laser-induced breakdown spectroscopy is a powerful analytical method, but LIBS is subject to a matrix effect which can limit its ability to produce quantitative results in complex materials such as geologic samples. Various methods of sample preparation, calibration, and data processing have been attempted to compensate for the matrix effect and improve LIBS precision. This study focuses on sample preparation by comparing fused glass as a preparation for powdered material to the more commonly used method of pressing powder into pellets for LIBS analysis of major elements in complex geologic materials. Pelletizing powdered material is a common and convenient method for preparing samples but problems with the physical matrix brought on by inconsistencies in the homogeneity, density, and laser absorption, coupled with the chemical matrix problem lead to spectral peak responses that are not always consistent with the absolute concentration of representative elements. Twenty-two mineral and rock samples were analyzed for eight major oxide elements. Samples were prepared under both glass and pellet methods and compared for internal precision and overall accuracy. Fused glass provided a more consistent physical matrix and yielded more reliable peak responses in the LIBS analysis than did the pressed pellet preparation. Statistical comparisons demonstrated that the glass samples expressed stronger separability between different mineral species based on the eight elements than for the pressed pellets and showed better spot-to-spot repeatability. Regression models showed substantially better correlations and predictive ability among the elements for the glass preparation than did those for the pressed pellets.

1. Introduction and background

This study compares fused glass to the more common pressed pellet method for preparing powdered geological materials for laser-induced breakdown spectroscopy (LIBS). The goal of the study is to determine if fused glass preparations can provide greater precision and yield better calibration models than can be generated with a pressed powder preparation. It was hypothesized that some issues associated with matrix problems such as compositional variation, inconsistent laser absorption, and inhomogeneity of pelletized powder could be reduced with the fused glass matrix.

Laser-induced breakdown spectroscopy is a well-established analytical method and new applications continue to arise. Among the most common applications is material quality control analysis in manufacturing and pharmaceutical settings [1–6]. Researchers have also applied LIBS to environmental and geologic studies [7–13], explosive detection [12] and forensic analysis [14–16]. The growing interest in LIBS over a wide range of applications stems from its unique advantages over other analytical methods in that it is relatively non-destructive, it can analyze composition at pin-point locations, and has a relatively low operating cost.

A significant drawback to the LIBS technique is its sensitivity to the matrix effect [17–20]. Since characteristics including the composition of the sample, its hardness, density, surface texture, and energy absorption can affect the analytical response [7,21], developing accurate and repeatable calibration methods can present challenges. Many examples of high degrees of accuracy and precision have been shown for analysis with LIBS, but many of those studies used materials with relatively simple compositions and limited ranges in concentration of elements of importance [4,5,22,23]. A particular problem for geologic materials is the chemical matrix effect which arises from the complexity and variability of the composition of natural samples and the large number of elements of interest [21,24,25]. The physical and chemical matrix issues associated with minerals and rocks can affect the laser coupling to the sample and the intensity of a spectral line in ways that are not directly related to the absolute abundance of the element associated with that peak, thus creating problems in the development of calibration curves [17]. Often calibration curves created with geologic materials, even those generated with a consistent matrix, do not produce the accuracy desired for quantitative studies [40].

Newer methods of calibration using chemometrics and calibration-free techniques have been presented [19,20,26–28] but the most

* Tel.: +1 319 273 2772; fax: +1 319 273 7103.
E-mail address: patrick.pease@uni.edu.

0584-8547/$ – see front matter © 2013 Elsevier B.V. All rights reserved.
http://dx.doi.org/10.1016/j.sab.2013.03.001

verifiable results for quantitative analysis are derived from a predictable correlation between element concentration and spectral response developed with external calibration standards. Accurate calibration is most readily accomplished with a closely matched matrix between standards and unknown samples; however, developing standards almost always requires a matrix that does not match the material being analyzed [20]. Usually, samples must be ground and processed in some way to conduct the independent analysis to determine the standard's composition. Typically, standards are developed from powdered material compressed into pellets [21,25,29] and subsets of those powders can then be independently analyzed with other methods such as INAA, ICP-MS, or XRF. However, the change in the physical matrix of the standard requires that unknown samples be prepared in the same way for the best quantitative accuracy. Geological standards are available, or can be produced relatively easily from rocks or minerals which provide the best chemical match for natural geologic materials. The nature of pelletized material, however, results in inconsistent spectral response and does not always produce peaks proportional to the element concentration [30]. Anzano et al. [21] noted this problem and identified loose powder on tape as an improvement over pressed pellets and Lal et al. [29] also noted how the pressure used to compress pellets affected the spectral response.

This study examines an alternative preparation method, fused glass, for LIBS analysis of geologic materials. The glass material approach does not solve the chemical matrix issue, but it does provide more stable physical matrix conditions, limits inconsistencies in laser absorption, reduces detector saturation on strong lines due to sample dilution, and provides an overall improved calibration over traditional pressed pellets. Multivariate calibration methods such as PCR and PLS can compensate for some calibration problems [18,25,31,39] and PLS models are examined in this paper; however, most of the analyses presented here are based on univariate models because the goal is to improve the calibration and quantification of geologic materials in the preparation and analysis stage of the study. Improvements at the beginning of the analytical procedure will then translate throughout the study enhancing the data analysis regardless of statistical treatments.

2. Materials and methods

2.1. Material description

Twenty-two samples were prepared and tested in this study; 9 samples were rock and 13 were mineral. This study primarily focused on the major oxide elements Al, Ca, Fe, K, Mg, Na, Si, and Ti, but some trace elements were also examined. The rock samples were USGS standard reference powders for which the elemental concentrations were known. These included five common rock types as well as a manganese nodule selected to represent a more exotic composition (Table 1). Three additional standards were made by mixing multiple powders into hybrid compositions. The 13 mineral samples selected for this study represent 12 common rock-building silicate minerals and the oxide mineral hematite (Table 1). The minerals were obtained from Ward's Natural Science as large specimen samples specifically for this study.

All samples were initially ground to a fine powder (the USGS rock samples were already powdered). The mineral samples were selected from single, large crystals of about 3 cm diameter. The crystals were initial pulverization and then were ground to a fine powder passing a 38 μ sieve. The finely ground powder was homogenized and split into lots. A subsample from each was weighed out and mixed with a graphite binding agent at a ratio of 90% sample to 10% binder. The materials were put in a glass vial and mixed with a tumbler for 1 h to ensure homogenization of the sample and binder. The mixed powder from each sample was then pressed into 1 cm diameter pellets at 3000 psi (21 MPa) using a hydraulic press and stainless steel die.

A second subsample from each lot was used to produce fused glass disks. A lithium borate flux was used at a 5:1 flux to sample ratio and fused at 1050 °C using Pt–Au crucibles and molds. All 22 samples were then analyzed with an XRF method to generate the baseline reference composition. Those composition values were used as the standard for the minerals used throughout this study. The USGS standards had known compositions and served as a quality check for the XRF results. Following the XRF analysis, the surface of the glass disks was

Table 1
List of rock and mineral samples used in the study with the concentrations of eight major elements.

	Major element concentrations %							
	Al	Ca	Fe	K	Mg	Na	Si	Ti
USGS rock standards								
Granodiorite	7.88	1.51	3.43	4.48	0.58	2.06	31.10	0.40
Basalt	7.16	8.17	8.63	0.43	4.36	1.64	23.30	1.63
Quartz latite	8.57	2.27	3.04	2.99	0.60	3.12	30.66	0.37
Shale	3.45	5.99	2.12	1.38	2.68	2.22	13.20	0.15
Diabase	8.18	7.76	7.58	0.52	3.84	1.63	24.68	0.64
Mn nodule	2.05	11.01	10.91	0.50	2.87	0.74	1.49	0.32
Mix 1	5.41	3.71	2.32	1.97	1.48	2.40	19.74	0.24
Mix 2	4.47	5.63	6.45	2.24	1.55	1.26	14.66	0.32
Mix 3	5.78	3.49	4.77	3.14	1.04	1.56	21.33	0.34
Inosilicates								
Actinolite	1.80	4.99	5.02	0.27	14.03	0.29	26.42	0.02
Augite	0.57	16.33	7.68	0.03	7.33	0.42	24.21	0.02
Diopside	0.85	14.33	3.08	0.08	12.30	0.24	24.64	0.05
Hornblende	0.89	4.73	5.00	1.70	11.37	3.94	25.81	0.15
Tectosilicates								
Albite	11.26	1.89	0.15	0.61	<0.03	7.94	29.67	
Anorthite	12.86	9.00	3.28	0.20	2.11	2.36	24.23	0.06
Microcline	9.83	0.07	0.42	11.26	<0.03	1.62	30.13	<0.01
Nepheline	18.12	0.37	0.28	4.46	<0.03	12.14	20.35	<0.01
Quartz	0.27	0.01	0.35	0.03	<0.03	<0.05	45.28	0.00
Chert (cryptocrys. qtz)	0.48	0.08	0.52	0.07	<0.03	<0.05	44.96	0.01
Phyllosilicate (mica)								
Muscovite	19.45	0.02	1.50	8.99	0.41	0.57	22.58	0.11
Nesosilicate								
Olivine	0.20	0.31	4.45	<0.01	25.84	0.08	22.89	0.00
Oxide								
Hematite	2.02	0.10	75.75	0.39	0.23	0.27	2.30	0.09
LIBS peaks used	396.2	445.5	375.0	766.5	518.4	818.3	288.2	336.1

frosted with silicon carbide abrasive then cleaned in preparation for LIBS analysis. In their original state, the glass disks were too transparent and the laser pulse penetrated deep into the glass causing laser ablation to occur below the surface.

2.2. Analytical methods

The LIBS instrumentation included an Nd:YAG (1064 nm), 150 mJ Litron laser, an Echelle spectrometer, and an EMCCE camera collecting wavelengths from 200 to 1000 nm at a 0.02 nm interval. Spectra were collected from each pellet and glass disk from 15 individual spots along a grid pattern with 1 mm spacing. Ten pulses were recorded and averaged at each spot. Ten of the results were used in ANOVA analyses and regression model development and the remaining five were used as validation. An example of LIBS spectra is shown in Fig. 1. Single peaks were used for each element to provide the simplest comparison of preparation methods and those peak values can be found in Tables 1, 2a, 2b, 2c, and 3a, 3b, 3c and in Figs. 2 and 3. The best peaks were chosen based on known wavelengths of importance for each element [34] and empirically by examining regression results to find the best results.

The plasma emission was substantially stronger for the pressed pellets than for the glass disks as a consequence of a difference in laser absorption and ablation rates (cf. Fig. 1). In order to compare the spectra of the two sample preparations, the baseline was removed and peaks were normalized to the total light of emission. Initial experiments were conducted to compare normalization to the background continuum which is related to the ablation rate [30] and normalization to the total emission. There was little variation between the two methods, although normalization to the total light produced slightly better calibrations for most cases.

This study removed the baseline continuum at each peak location prior to normalization [cf. 32], because the baseline is related to the continuum fluorescence [cf. 33] and empirical experiments showed a slight improvement in results. Baseline identification was accomplished with

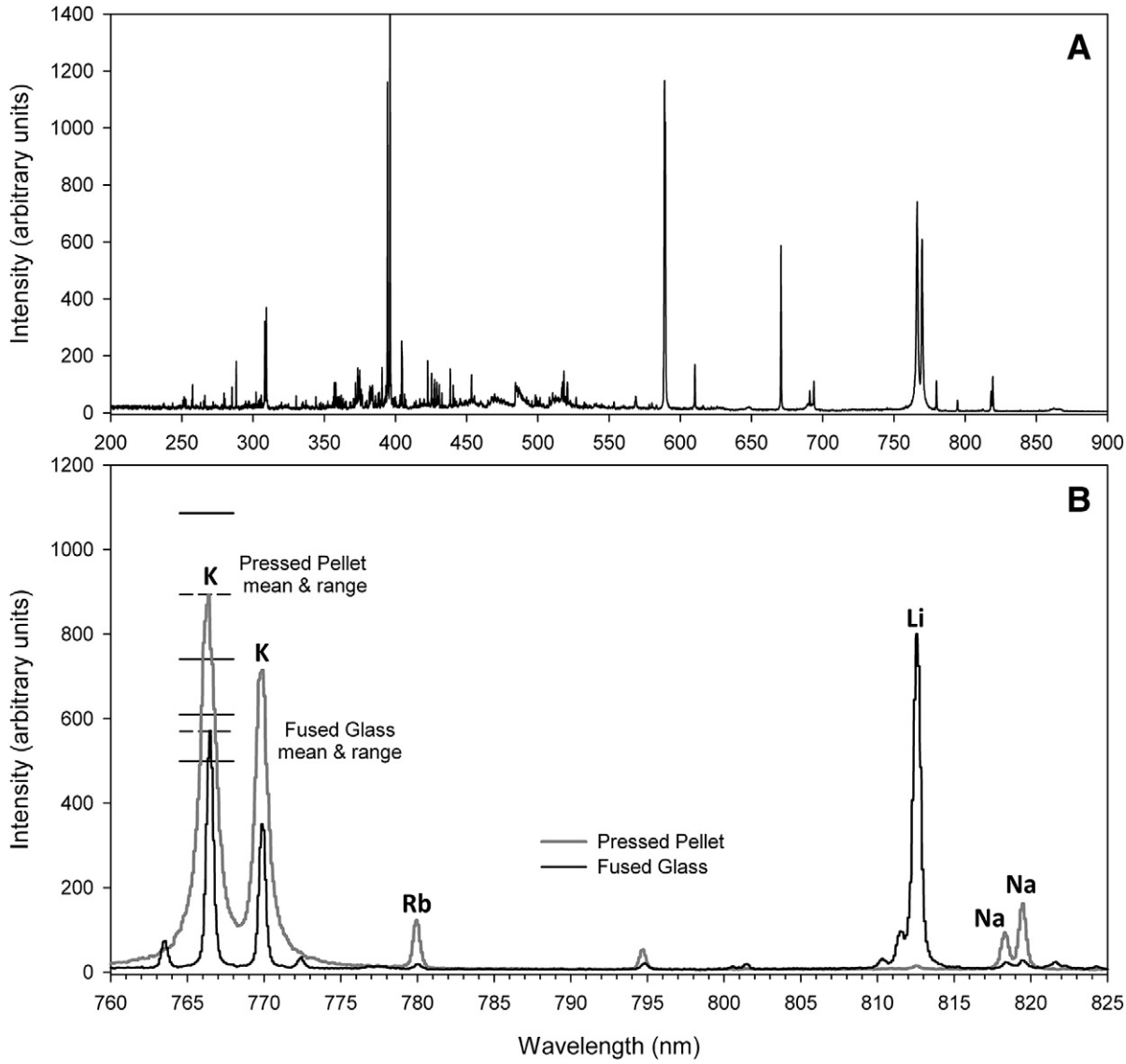

Fig. 1. Example of LIBS spectra. Part A shows the full spectrum of a muscovite sample. Part B shows an enlarged section in the regions of the K 766.49 line used in this study for both glass and pellet samples. The spectra lines in part B are the composite average of all 10 spectra collected from different spots on the muscovite samples to make the lines easier to see. The gray boxes represent mean and ranges for the 10 spectra on each sample type for the K 766.49 line. The better spot-to-spot repeatability of the fused glass compared to the pressed pellet is apparent by the narrower minimum–maximum range for the glass. The fused glass samples present a lower overall intensity on individual peaks due to the dilution of sample with flux. Also note the large Li peak for the fused glass sample resulting from the lithium borate flux used in the preparation.

Table 2a
ANOVA results for 22 rock and mineral samples prepared as fused glass disks.

	One-way ANOVA	Sum of squares	df	Mean square	F	Sig.	ω^2
Al	Between groups	9.34E−02	21	4.45E−03	1169.1	0.000	0.991
	Within groups	7.53E−04	198	3.80E−06			
	Total	9.42E−02	219				
Ca	Between groups	1.43E−02	20	7.13E−04	683.816	0.000	0.986
	Within groups	1.87E−04	179	1.04E−06			
	Total	1.44E−02	199				
Fe	Between groups	1.45E−03	18	8.05E−05	526.698		0.982
	Within groups	2.34E−05	153	1.53E−07			
	Total	1.47E−03	171				
K	Between groups	2.70E−03	21	1.29E−04	495.879	.000	0.980
	Within groups	5.04E−05	194	2.60E−07			
	Total	2.75E−03	215				
Mg	Between groups	2.36E−02	16	1.47E−03	2226.034	.000	0.995
	Within groups	9.54E−05	144	6.63E−07			
	Total	2.37E−02	160				
Na	Between groups	2.71E−04	17	1.94E−05	166.144	.000	0.965
	Within groups	8.65E−06	97	7.86E−08			
	Total	2.80E−04	114				
Si	Between groups	1.01E−02	21	4.45E−03	120.207	.000	0.919
	Within groups	7.96E−04	198	4.02E−06			
	Total	1.09E−02	219				
Ti	Between groups	2.12E−04	13	1.63E−05	83.781	.000	0.895
	Within groups	2.18E−05	112	1.95E−07			
	Total	2.34E−04	125	4.45E−03			

a two-stage, sliding window, low-pass filter developed for this study which took the form of

$$B_i = \frac{1}{n}\sum_{P=i-n/2}^{P+n-1} P_m$$
$$P_m = {}_{min}P_{k=i-m/2}^{k+m-1} \quad \{P_m \in k | P_m < \mu, P_m \not< \mu \rightarrow P_m = \mu\} \tag{1}$$

where B_i is the baseline value at location i, n and m *are* the window sizes for passes P and k, and μ is the spectrum mean.

3. Results

3.1. ANOVA

A one-way ANOVA was carried out to examine the degree of separability between samples that could be achieved based on element identification under each of the two preparation methods (Tables 2a and 3a). The goal was to confirm that the individual rock/mineral samples could be distinguished from one another based on the spectral response associated with major elements under both sample preparation methods and to compare the relative strength of the separability achievable under both methods.

Table 2b
Welch and Brown–Forsythe statistic for 22 rock and mineral samples prepared as fused glass disks.

		Statistic	df1	df2	Sig.
Al	Welch	1877.30	21	71.89	.000
	Brown–Forsythe	1169.10	21	58.34	
Ca	Welch	852.13	20	64.60	.000
	Brown–Forsythe	720.16	20	103.65	
Fe	Welch	238.31	16	57.33	.000
	Brown–Forsythe	578.81	16	50.79	
K	Welch	922.73	21	70.62	.000
	Brown–Forsythe	506.49	21	18.76	
Mg	Welch	1437.25	16	37.51	.000
	Brown–Forsythe	2360.75	16	40.89	
Na	Welch	94.75	16	21.65	.000
	Brown–Forsythe	264.10	16	23.37	
Si	Welch	442.00	21	71.69	.000
	Brown–Forsythe	120.21	21	59.69	
Ti	Welch	90.68	13	36.98	.000
	Brown–Forsythe	77.23	13	21.20	

The results of the ANOVA indicate that the null hypothesis should be rejected in favor of the alternative that there are significant differences between the spectral peak responses for all eight major elements among the 22 samples under both preparations of glass disks and pressed pellets (Tables 2a and 3a). Individually, the F ratios are large for different elements and the significance levels are well below 0.05 in all cases for both the fused glass and pressed pellet samples (Tables 2a and 3a). This indicates that the variance in the spectral responses of each element was significantly larger between different rock/mineral types, than was the spot-to-spot variance within each sample. As a secondary check on the ANOVA validity, a Kruskal–Wallis test on ranks was also conducted. Kruskal–Wallis is a non-parametric test which does not assume normality. The null hypothesis that samples are from identical populations was rejected in all cases because significance levels were consistently below 0.05. The results of the Kruskal–Wallis test are included in Tables 2c and 3c.

The ANOVA assumes that samples are normally distributed and exhibit homogeneous variance. Since the multiple probe locations on a single sample do not really represent a random population, a Shapiro–Wilk test was performed for the 10-shot runs prior to other analyses to ensure that the basic assumptions of normality were met. The results of the Shapiro–Wilk test of normality indicated that the assumptions of normality were met for all but 10 of the 176 cases (eight elements across 22 samples) for samples prepared as fused glass. For pressed pellet samples, 22 of the 176 cases failed the test of normality which was a failure rate twice as high as for samples prepared as fused glass. This higher rate of non-normality is attributed to a lower level of spot-to-spot repeatability in the pressed pellets.

Homogeneity of variance was also analyzed prior to ANOVA using the Levene statistic. Results for the Levene's test revealed p-values that were below the 0.05 significance level for all elements in both the fused glass and pressed pellet preparations, meaning the equal variance assumption was violated. Even though this failed the test of homogeneity, ANOVA is generally robust to the violation so long as group sizes are equal. However, some elements showed no peaks in some samples, thus creating differing group sizes in the final analysis that potentially created problems in the ANOVA. To compensate for this, adjusted F statistics using Welch and Brown–Forsythe robust tests of equality of means were also carried out and reported. The adjusted F statistics provide good alternative values when the assumption of homogeneity has been violated. The separability demonstrated by the one-way ANOVA is supported by the adjusted F values in both the Welch and Brown–Forsythe tests (Tables 2b and 3b) and by the H values in the non-parametric Kruskal–Wallis test (Tables 2c and 3c). Although this was the expected result, it does confirm the ability to distinguish mineral types based on each of the eight major elements examined in this study.

3.2. Omega square

The ANOVA results provide strong conformation of general separability of mineral and rock species based on major elements; however, the results are difficult to compare across mineral and treatment types due to scaling issues. The glass and pressed pellets yielded different absolute values due to the higher ablation rates on the pressed pellet as well as the dilution of sample in the glass flux. Therefore, the sum of squares across different samples and preparation methods is not directly comparable in an absolute value. Likewise, within a single sample the range of different elements produces widely differing peak values across the spectrum that are not directly related to one another. To get around this issue, and to get a better idea of the strength of the ANOVA results, an effect size can be used to make the data more comparable across samples. Omega squared is an unbiased effect size indicator for between-group analysis used to estimate

Table 2c
Kruskal–Wallis test results for 22 rock and mineral samples prepared as fused glass disks.

	Al	Ca	Fe	K	Mg	Na	Si	Ti
Chi-square	215.63	196.84	171.25	212.03	168.26	112.38	190.66	126.32
df	21	21	21	21	21	21	21	21
Asymp. sig.	.000	.000	.000	.000	.000	.000	.000	.000

the proportion of variance attributable to differences between the mineral types rather than within-sample variance. Omega squared is given as:

$$\omega^2 = \frac{SS_B - (df_B)(MS_W)}{SS_t + MS_W} \quad (2)$$

where SS_B = sum of squares between-group variation, MS_W = mean square within-group variation, SS_t = sum of squares total, and df = between-group degrees of freedom.

The effect size for all elements in both preparation methods is rather large (Tables 2a and 3a) and the effect size indicates that mineral samples can be separated based on spectral data at the chosen lines. The mineral types provide a wide range of spectral peaks, but the within group sum of squares remains relatively low due to good spot-to-spot repeatability. The low within group variance compared to the much larger between group variability results in a high effect size.

3.3. Post hoc test

ANOVA provides a strong case for the separability of minerals and rocks based on the spectral results of major elements in glass disks and it is useful to see the strength of the relationship between the variables provided by the effect size. However, those results primarily indicate the degree to which differences exist within elemental responses between samples; they provide little information for where the differences occur or the overall data trends. To get a better idea of the structure of the data, a Games–Howell post hoc test for multiple comparisons was conducted to show the difference between individual samples. The Games–Howell test does not require equal variance and provides a cross-comparison of each sample with the 21 other samples for each of the eight elements. In nearly all cases, there was a significant difference in the instrument response between each sample for all eight major elements. The data tables are too extensive to include in this paper, but 92% of the 1790 cross-comparisons for the fused glass samples, and 92% of 1841 cross-comparisons for pressed pellets, showed differences in spectral peak response at the 0.05 significance level when doing sample-to-sample comparisons of each of the eight elements. The maximum number of possible cross tabulations was 1848 and the lower case numbers here result from some elements yielding no peak in some samples. In the vast majority of cases where rocks/minerals were not distinguishable from one another based on an individual element response, it was because the samples had similar concentrations of that element. For example, a comparison of the basalt and granodiorite samples showed that all eight major elements exhibit significant differences and can be distinguished in glass and pellet form. Conversely, the spectral results of Ca and Fe between the actinolite and hornblende samples were not significantly different due to the similarity in actual concentrations (4.99%–4.73% and 5.02%–5.0% respectively) of those elements in both samples. The high rate of significant differences across the 22 samples and eight element cross-comparisons indicated that in most cases minerals can be distinguished and classified based on LIBS results of one or more of the eight elements. In all cases, sample species were distinguishable based on at least three elements and about 90% were separable on at least six elements.

Table 3a
ANOVA results for 22 rock and mineral samples prepared as pressed pellets.

	One-way ANOVA	Sum of squares	df	Mean square	F	Sig.	ω^2
Al	Between groups	0.2228	21	0.0106	605.304	.000	0.983
	Within groups	0.0035	198	0.0000			
	Total	0.2263	219				
Ca	Between groups	0.1144	21	0.0054	720.356	.000	0.986
	Within groups	0.0015	197	0.0000			
	Total	0.1158	21				
Fe	Between groups	0.0041	21	0.0002	126.878	.000	0.923
	Within groups	0.0003	198	0.0000			
	Total	0.0045	219				
K	Between groups	0.0251	21	0.0012	1190.534	.000	0.991
	Within groups	0.0002	198	0.0000			
	Total	0.0253	219				
Mg	Between groups	0.1714	19	0.0090	1320.477	.000	0.992
	Within groups	0.0012	178	0.0000			
	Total	0.1726	197				
Na	Between groups	0.0064	18	0.0004	954.961	.000	0.989
	Within groups	0.0001	170	0.0000			
	Total	0.0065	188				
Si	Between groups	0.0602	21	0.0029	613.849	.000	0.983
	Within groups	0.0009	198	0.0000			
	Total	0.0611	219				
Ti	Between groups	0.0005	18	0.0000	103.968	.000	0.915
	Within groups	3.73E−05	153	0.0000			
	Total	0.0005	171	0.0106			

3.4. Coefficient of variation

Based on the ANOVA and post hoc tests, both preparation methods are appropriate for distinguishing major elements in geologic samples as the between-sample means and variations are much larger than the single sample error. An additional measure of relative accuracy of the two preparation methods for bulk analysis of geologic material is the coefficient of variation (Cv). The Cv is a normalized, non-dimensional measure of the standard deviation. The coefficient of variation is expressed as a percent and is the ratio of the standard deviation and the average of each element in each sample type, such that $Cv = \sigma/\bar{x}$, where σ = standard deviation and $\bar{x}$ = sample mean. Representing the variance as a percent of the mean removes the bias of scale in absolute concentration and is useful here because of the variation in signal strength between the diluted glass samples

Table 3b
Welch and Brown–Forsythe statistic for 22 rock and mineral samples prepared as pressed pellets.

		Statistic	df1	df2	Sig.
Al	Welch	810.60	21	71.72	.000
	Brown–Forsythe	605.30	21	65.98	
Ca	Welch	1761.35	21	70.86	.000
	Brown–Forsythe	724.13	21	137.11	
Fe	Welch	229.42	21	72.19	.000
	Brown–Forsythe	126.88	21	86.59	
K	Welch	1008.14	21	71.58	.000
	Brown–Forsythe	1190.53	21	83.51	
Mg	Welch	960.51	19	65.40	.000
	Brown–Forsythe	1335.76	19	70.63	
Na	Welch	938.81	18	61.78	.000
	Brown–Forsythe	960.83	18	64.51	
Si	Welch	321.69	21	72.00	.000
	Brown–Forsythe	613.85	21	52.07	
Ti	Welch	167.68	18	49.44	.000
	Brown–Forsythe	110.90	18	44.17	

Table 3c
Kruskal–Wallis test results for 22 rock and mineral samples prepared as pressed pellets.

	Al	Ca	Fe	K	Mg	Na	Si	Ti
Chi-square	215.30	212.60	198.64	214.09	191.60	184.76	208.05	155.02
df	21	21	21	21	19	18	21	18
Asymp. sig.	.000	.000	.000	.000	.000	.000	.000	.000

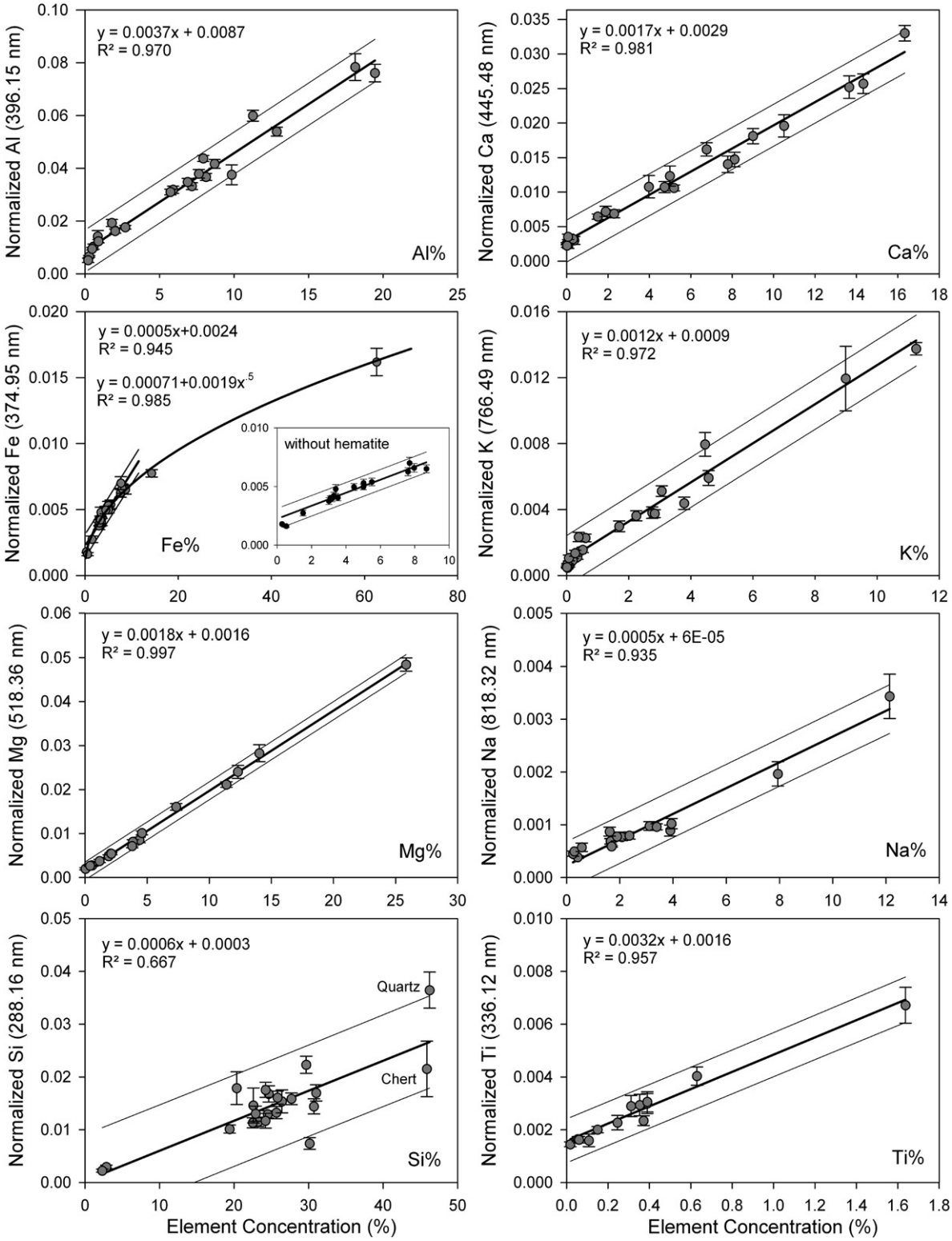

Fig. 2. Linear regression models for eight major elements from 22 rock and mineral samples prepared as fused glass. Regression and 95% prediction lines are shown. Error bars are standard deviation of the spot-to-spot variations.

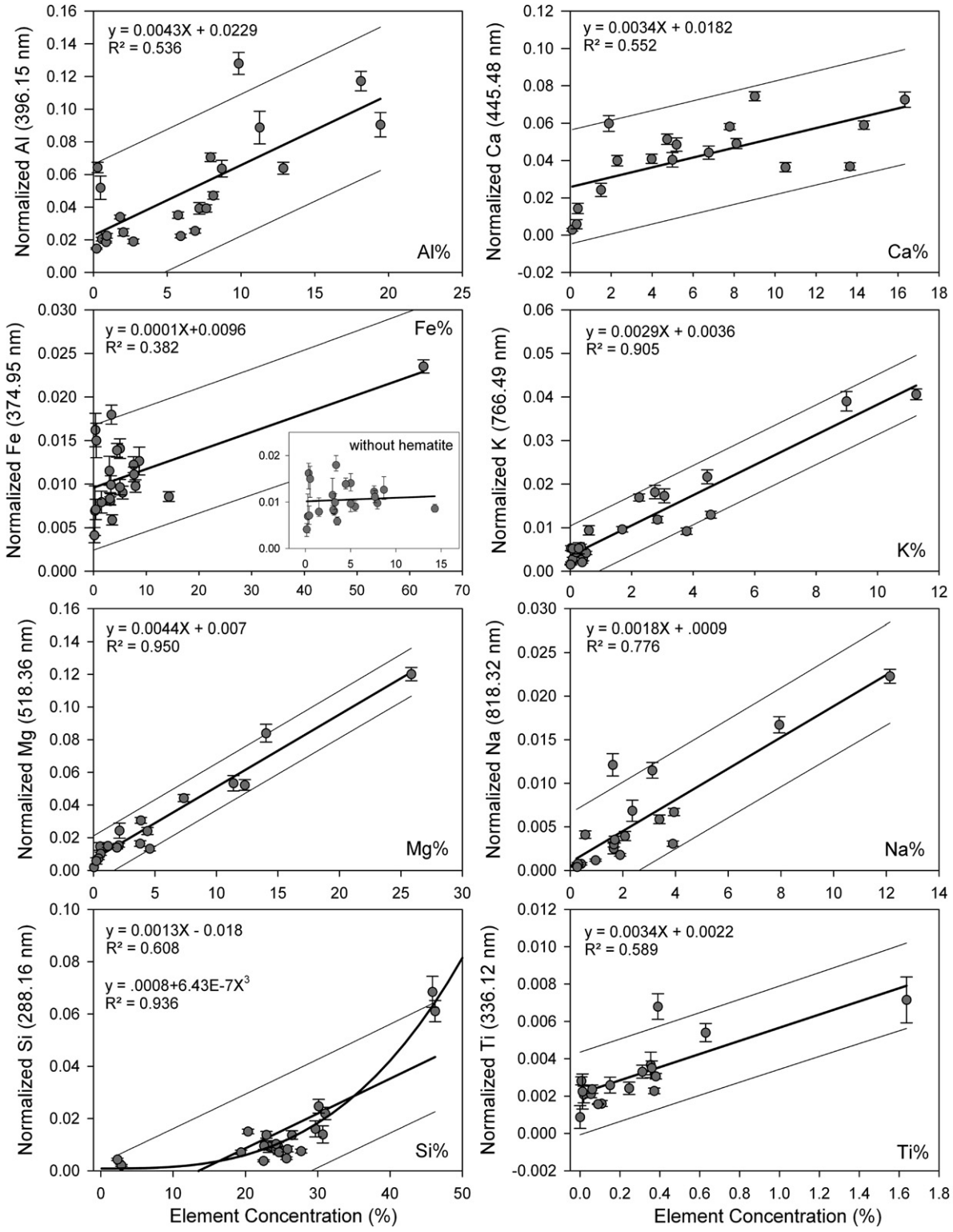

Fig. 3. Linear regression models for eight major elements from 22 rock and mineral samples prepared as pressed powder pellets. Regression and 95% prediction lines are shown. Error bars are standard deviation of the spot-to-spot variations.

and the powder of the pressed pellets. Importantly, the coefficient of variation is an expression of the precision of repeated measurements on the same sample and, since it is a dimensionless number, allows comparisons of precision between differing samples.

Although both fused glass and pressed pellet preparations show good separability between sample types in the ANOVA and post hoc test, *Cv* elucidates a significant difference in the repeatability of multiple shots on a single sample (Tables 4 and 5). The fused glass preparation yielded better spot-to-spot repeatability between the 10 different shot locations as shown by generally smaller *Cv* compared to the pellets. The improved repeatability on glass samples over the pellet preparation indicates either more consistent matrix conditions

Table 4
Coefficient of variation results for rock and mineral samples prepared as fused glass disks. Missing data are cases where the concentration was below the detection limits of the XRF method or where no peak was generated in the analysis. Values in bold font denote row and column means.

	Coefficient of variation — glass disks								
	Al	Ca	Fe	K	Mg	Na	Si	Ti	Mean
Granodiorite	2.6%	5.7%	7.9%	7.6%	6.2%	8.5%	9.1%	9.1%	**7.1%**
Basalt	3.9%	7.1%	5.3%	9.9%	7.3%	7.0%	7.8%	9.1%	**7.2%**
Quartz latite	4.0%	8.6%	7.7%	6.3%	7.7%	14.1%	9.9%	13.8%	**9.0%**
Shale	4.4%	8.2%	6.7%	8.4%	4.4%	14.1%	8.4%	12.2%	**8.3%**
Diabase	3.6%	8.5%	5.5%	9.1%	5.9%	11.3%	5.4%	8.7%	**7.1%**
Mn nodule	3.9%	6.5%	3.6%	12.5%	5.8%	3.9%	10.8%	7.9%	**6.9%**
Mix 1	4.3%	4.1%	6.7%	9.1%	2.3%	9.3%	7.0%	13.7%	**7.2%**
Mix 2	3.4%	6.0%	5.5%	6.3%	6.4%	7.3%	7.6%	12.7%	**6.9%**
Mix 2	4.0%	15.1%	6.1%	8.5%	9.6%	12.6%	8.8%	12.5%	**9.6%**
Nepheline	6.5%	19.3%	–	9.0%	–	11.3%	17.4%	–	**12.7%**
Augite	9.8%	3.4%	6.9%	9.0%	4.6%	–	12.1%	6.4%	**7.5%**
Diopside	15.7%	5.5%	5.3%	9.3%	6.2%	–	9.2%	57.9%	**15.6%**
Albite	3.4%	9.8%	–	9.8%	–	17.5%	7.3%	–	**9.4%**
Anorthite	3.1%	6.0%	7.2%	9.6%	5.1%	5.8%	8.2%	7.7%	**6.6%**
Quartz	4.9%	6.9%	–	6.8%	–	–	9.4%	–	**7.0%**
Chert	4.9%	22.3%	–	16.4%	–	–	24.4%	–	**17.0%**
Actinolite	6.9%	9.8%	6.0%	13.8%	6.8%	–	14.2%	–	**9.6%**
Hornblende	5.1%	7.5%	4.8%	9.8%	3.0%	8.5%	7.7%	6.0%	**6.6%**
Muscovite	4.4%	9.6%	9.0%	16.4%	4.1%	5.0%	22.7%	15.0%	**10.8%**
Hematite	4.7%	–	6.2%	–	–	–	13.0%	–	**8.0%**
Olivine	15.8%	9.8%	5.8%	6.8%	3.1%	–	11.0%	–	**8.7%**
Microcline	9.8%	9.7%	–	2.8%	–	5.3%	15.0%	–	**8.5%**
Mean	**5.9%**	**9.0%**	**6.2%**	**9.4%**	**5.5%**	**9.4%**	**11.2%**	**13.8%**	

or better homogenization, or a combination of both. Most of the individual element repeatability for the 22 samples of fused glass had variations less than 10% of the mean. Of the 148 values in Table 4, 80% had standard deviations within 10% of the mean. The majority of cases where the *Cv* was higher were associated with oxide concentrations below 1% in the sample which means that the actual oxide concentration in the glass was less than 0.2%, due to flux dilution, and the actual element concentration was still lower than that. Examining the individual element data collected from the fused glass samples, six of the eight major elements exhibited average repeatability within 10% of the mean across the 22 different sample types (columns in Table 4). Si and Ti showed the weakest repeatability across the different samples, with mean values of 11.2% and 13.8%, but in general the repeatability was good. Likewise, when examining the rock/mineral types, a relatively high precision was observed across the eight different elements for most of the different sample types (rows in Table 4). Eighteen of the 22 different samples exhibited mean deviations within 10% of the sample mean across all eight elements. Chert showed the largest variability in spot-to-spot response at 17% of the mean, which was much higher than observed for the crystalline quartz. Even in cases that presented high *Cv*, most individual elements still yielded good results. For example, diopside had a high *Cv* that was mostly a consequence of the poor repeatability for the Ti line. Likewise, although muscovite had a mean *Cv* of 10.8%, a much lower individual *Cv* was observed for Al, Fe, Mg, and Na.

Table 5
Coefficient of variation results for rock and mineral samples prepared as pressed pellets. Values in bold font denote row and column means.

	Coefficient of variation — pressed pellets								
	Al	Ca	Fe	K	Mg	Na	Si	Ti	Mean
Granodiorite	3.7%	14.6%	6.0%	6.1%	16.1%	13.5%	10.6%	10.1%	**10.1%**
Basalt	9.1%	5.6%	12.6%	22.0%	9.0%	24.5%	23.9%	17.2%	**15.5%**
Quartz latite	8.0%	7.0%	14.4%	9.3%	9.6%	7.8%	23.4%	18.6%	**12.3%**
Shale	5.2%	6.7%	9.9%	4.8%	10.6%	10.0%	9.7%	13.5%	**8.8%**
Diabase	4.9%	2.8%	7.5%	9.0%	5.8%	10.1%	13.0%	9.0%	**7.8%**
Mn nodule	7.3%	5.3%	6.6%	10.9%	10.4%	11.2%	17.0%	6.5%	**9.4%**
Mix 1	5.7%	7.4%	5.9%	8.4%	7.7%	8.6%	9.6%	10.6%	**8.0%**
Mix 2	5.6%	8.0%	7.3%	6.1%	6.8%	11.1%	11.3%	10.5%	**8.3%**
Mix 2	5.3%	6.0%	8.2%	7.8%	6.1%	8.1%	10.3%	4.8%	**7.1%**
Nepheline	5.1%	19.1%	41.0%	7.4%	–	3.5%	6.0%	–	**13.7%**
Augite	5.6%	5.6%	7.5%	18.7%	4.9%	17.2%	8.4%	6.3%	**9.3%**
Diopside	3.0%	3.9%	8.3%	12.6%	6.3%	5.2%	11.9%	9.6%	**7.6%**
Albite	11.3%	7.1%	21.2%	11.4%	–	5.6%	19.3%	6.1%	**11.7%**
Anorthite	5.7%	3.3%	10.3%	16.9%	19.0%	17.7%	10.2%	9.5%	**11.6%**
Quartz	5.0%	37.1%	11.8%	10.5%	–	–	6.6%	7.6%	**13.1%**
Chert	13.7%	32.8%	13.2%	12.4%	–	–	8.7%	41.8%	**20.4%**
Actinolite	3.5%	9.6%	8.0%	24.2%	6.4%	16.8%	11.8%	5.6%	**10.8%**
Hornblende	6.5%	5.5%	9.3%	6.5%	8.9%	6.2%	13.2%	16.4%	**9.1%**
Muscovite	8.3%	11.2%	15.8%	5.7%	10.1%	10.4%	14.6%	9.7%	**10.7%**
Hematite	8.9%	25.1%	3.2%	–	33.5%	11.4%	10.8%	1.5%	**13.5%**
Olivine	3.1%	41.7%	5.7%	8.5%	3.4%	–	9.5%	–	**12.0%**
Microcline	5.3%	24.4%	16.4%	3.0%	–	10.5%	10.6%	–	**11.7%**
Mean	**6.3%**	**13.2%**	**11.4%**	**10.6%**	**10.3%**	**11.0%**	**12.3%**	**11.3%**	

The coefficient of variation for samples prepared as pressed powder pellets exhibited notably less precision. Only 63% of cases shown in Table 5 yielded repeatability within 10% of the sample mean. Dilution is not an issue for the pressed pellet analysis. Al, with a mean *Cv* of 6.3%, was the only individual element that exhibited a consistently low *Cv* across the 22 different samples. Ca and Si yielded the highest variability, with average *Cvs* of 13.2% and 12.3%. Examining the different rock/mineral types, the different sample species also showed high amounts of variability when considering all eight elements together. Thirteen of the 22 sample types had an average *Cv* greater than 10% across the eight major elements, with chert and basalt showing the poorest precision. Once again, chert was the most problematical sample. The average variation from the sample mean was over 20%, with Ti and Ca contributing much of the variability. It is not clear why chert produced such poor repeatability under both preparation methods, especially as compared to quartz; however, the large variation in peak response between the two likely points to the importance of compositional and textural characteristics during the LIBS process. Macrocrystalline quartz, such as the sample used in this study, typically forms either through crystallization in silica-rich magma or in a hydrothermal environment. Chert is a microcrystalline or cryptocrystalline rock formed from saturated water in marine sedimentary environments. It is likely that the textural differences between the crystalline structure of quartz and chert resulted in variations in laser absorption and ablation characteristics [35]. Likewise, although samples used here had nearly identical SiO_2 concentrations (98.1% and 98.4%), chert is expected to have a more heterogeneous trace element composition than quartz; a characteristic which might suggest the importance of the chemical matrix to SiO_2 [21,34], even with small concentrations of interfering elements.

3.5. Regression models

Although the ANOVA and coefficient of variation analyses provide useful evidence of the ability to accurately distinguish compositional variation in geologic samples based on spectral signatures and consideration of the coefficient of variation demonstrates that the glass disks provide greater precision than do the pressed pellets, those methods do not provide predictive models or explain the structure of the correlations. For that, regression analyses were conducted.

Regression models provide the clearest evidence that the fused glass preparation improves accuracy and repeatability compared to the pressed powder for bulk analysis of geologic materials by LIBS. Tables 6 and 7 and Figs. 2 and 3 show the regression results for each of the eight major elements based on the spectral line with the highest coefficient of determination. Peaks used for the regression were chosen based on known wavelengths of importance for each element [34] and by empirical examination to find the best results. Each regression model was built using 220 data point consisting of peaks from 10 different spot locations on each of the 22 mineral and rock samples. The mean peak intensity of the 10 different spot locations was used for the regression value whereas the range of values for the 10 different spots was used to determine the spot-to-spot variance and is represented in the standard deviation error bars in Figs. 2

Table 6
Regression model results for fused glass disks. SEE = standard error of the estimate.

Element (peak)		Model summary		Coefficient			
		R^2	SEE	B	Std. Error	t	Sig.
Al	(396.15 nm)	.970	.0037	.004	1.5E−4	25.51	.000
Ca	(445.48 nm)	.981	.0012	.002	5E−5	31.69	.000
Fe[a]	(374.95 nm)	.945	.0005	.002	6.8E−5	16.63	.000
Fe[b]	(374.95 nm)	.985	.0004	.020	.001	16.21	.000
K	(766.49 nm)	.972	.0006	.001	4E−5	26.57	.000
Mg	(518.36 nm)	.997	.0007	.002	3E−5	70.58	.000
Na	(818.32 nm)	.955	.0002	2.4E4	1.3E−5	17.84	.000
Si	(288.16 nm)	.667	.0041	.001	9E−5	6.33	.000
Ti	(336.12 nm)	.957	.0003	.004	2.2E−4	16.35	.000

[a] Linear regression without hematite.
[b] Non-linear regression with hematite.

and 3. Both the regression model and the R^2 are shown on each plot. The models for major elements produced from the fused glass samples were better in every case than those produced from the pressed pellets. With the exception of Si, models produced from fused glass maintained R^2 values above 0.93. Likewise, the standard error of estimate (SEE), F-value, and t-statistic all indicate a strong model correlation (Table 6). The t-statistic tests the null hypothesis that the coefficient, or regression slope, is zero. It is the estimated coefficient of the model divided by the standard error which is an estimate of the standard deviation. The t-statistic suggests the number of standard deviations the coefficient value deviates from zero and is a measure of confidence that the independent variable can predict the dependent. Values of t above 2–3 are generally considered significant and with the exception of Si, t-statistic values for fused glass samples were 5 to 30 times higher.

Regression results from the pressed pellets showed notable lower predictive ability across the eight major elements. Only K, Mg, and the non-linear Si model achieved R^2 values above 0.9. Although the models generated from the pressed pellets were significant at the 0.05 confidence level (except for the Fe model without hematite), the t-values were near or below the acceptable threshold in all cases except K and Mg.

Mg produced the strongest model results under both preparation methods, although the resolution at low Mg concentrations produced problems within the pressed pellet samples. The low concentration problem with Mg for pressed pellets can also be seen in the coefficient of variation results in Table 5. In cases where the concentration was low, the shot-to-shot variation became large relative to the actual sample mean such as with granodiorite, hematite, and anorthite samples (Tables 1 and 5). The Mg results for the fused glass were excellent. The shot-to-shot variations remained more consistent in the fused glass (Table 4) and thus the issue of resolution at the low end was not a problem despite the dilution factor (Fig. 2).

Tables 6 and 7 provide regression results for Fe both with and without the hematite sample included because of its strong pull on the results which is clearly demonstrated in Figs. 2 and 3. The Fe model for the pressed pellets was poor regardless of the inclusion of hematite. When hematite was retained in the model the regression was significant (Table 7), but the examination of the plot in Fig. 3 reveals it as an outlier which pulled the results. In addition to its high concentration, hematite might not be compatible in this study because the iron in hematite is in an oxide form and thus has a different matrix than Fe bonded in a silicate structure. Once hematite was removed from the regression for the pressed pellets (Fig. 3, Table 7), there was no correlation and the slope essentially becomes zero (see t-value, Table 7) pointing to problems with Fe other than the hematite bonding. Problems with Fe calibration have been noted in studies of steel alloys and were attributed to matrix effects due to fractionation of Fe in the presence of other elements such as Zn [41,42]. St-Onge and Sabsabi [41] also reported that Fe peak intensities were smaller for pressed pellet samples made from powdered iron as compared to solid alloy standards. The reduced intensities were attributed to matrix effects associated with porosity in the pellet samples and the lack of fused or intermetallic crystal structures in the pellets [41].

Iron regression results for the fused glass preparation produced a substantially better fit compared to the pressed pellets (Fig. 2). Hematite still created problems with the signal response as demonstrated by the non-linear relationship. The non-linear response was likely caused by self-absorption due to the very high Fe concentration in hematite, which has been reported in other studies [41,34]. Using Fe results only from the lower concentration, silicate bonded minerals/rocks yielded an improved correlation for the remaining fused glass samples with an R^2 of 0.95. Given the substantially improved regression results, it appears that the fused glass method circumvented most of the physical matrix effects that plagued the pressed pellet samples and, possible, reduced fractionation issues associated with iron [41,42]. Also, if the hematite anomaly in the fused glass samples is the result of self-absorption, it suggests that the method may mitigate the issue of oxide versus silicate bonding although additional study is needed for confirmation. Regardless, the different results for Fe among the two preparations shown in Figs. 2 and 3 provide an excellent example of the importance of differences in the physical and chemical matrices during LIBS analysis.

Si results were problematic for both types of preparation. Linear models produced unacceptable results in both the fused glass and pressed pellet preparation. A non-linear model is also presented for the pressed pellet samples but, despite its high R^2 and significance level (Table 7), the value of the model is highly suspect because the trend is controlled by the very low and very high concentration samples. The majority of samples in the middle ranges are randomly scattered. The poor calibration of Si in both preparations, across all mineral types, likely resulted from problems associated with the Si bond strength effect on ablation and issues of self-absorption in the plasma [34,35]. Textural and compositional differences between quartz and chert were discussed above, but those do not fully explain the poor repeatability demonstrated among all mineral types used in this study. The Si results were not similar to some other regression attempts reported in the literature. For example, Anzano et al. [21] reported SiO_2 regressions with R^2 above 0.97 for pelletized artificial mixes. Similarly, Mohamed [36] reported SiO_2 calibrations with R^2 above 0.99. In both of those cases, however, the Si concentrations were relatively low; it did not exceed 10% in the Mohamed study and remained below 2% in the Anzano et al.'s study. Silicon concentrations in this study clustered between 20% and 30% (42%–64% SiO_2). This suggests that the chemical matrix problem is especially acute for high concentrations of Si. It is likely that Si correlations are better at a low concentration but at a higher concentration expected in silicate minerals, calibration might remain difficult.

Table 7
Regression model results for pressed powder pellets. SEE = standard error of the estimate.

Element	(Peak)	Model summary		Coefficient			
		R^2	SEE	B	Std. error	t	Sig.
Al	(396.15 nm)	.536	.0201	.004	.001	4.70	.005
Ca	(445.48 nm)	.552	.0161	.003	.001	4.96	.005
Fe[a]	(374.95 nm)	.006	.0036	7.6E−5	2.3E−4	0.33	.745
Fe[b]	(374.95 nm)	.382	.0036	2.1E−4	.6E−5	3.52	.000
K	(766.49 nm)	.905	.0034	.003	2.5E−4	13.83	.004
Mg	(518.36 nm)	.950	.007	.004	2.6E−4	16.92	.005
Na	(818.32 nm)	.776	.0029	.002	2.3E−4	7.68	.002
Si[c]	(288.16 nm)	.617	.0107	.001	2.3E−4	5.68	.002
Si	(288.16 nm)	.936	.0044	6.4E−7	3.8E−8	17.12	.000
Ti	(336.12 nm)	.589	.0010	.003	.001	5.22	.005

[a] Linear regression without hematite.
[b] Linear regression with hematite.
[c] Non-linear regression.

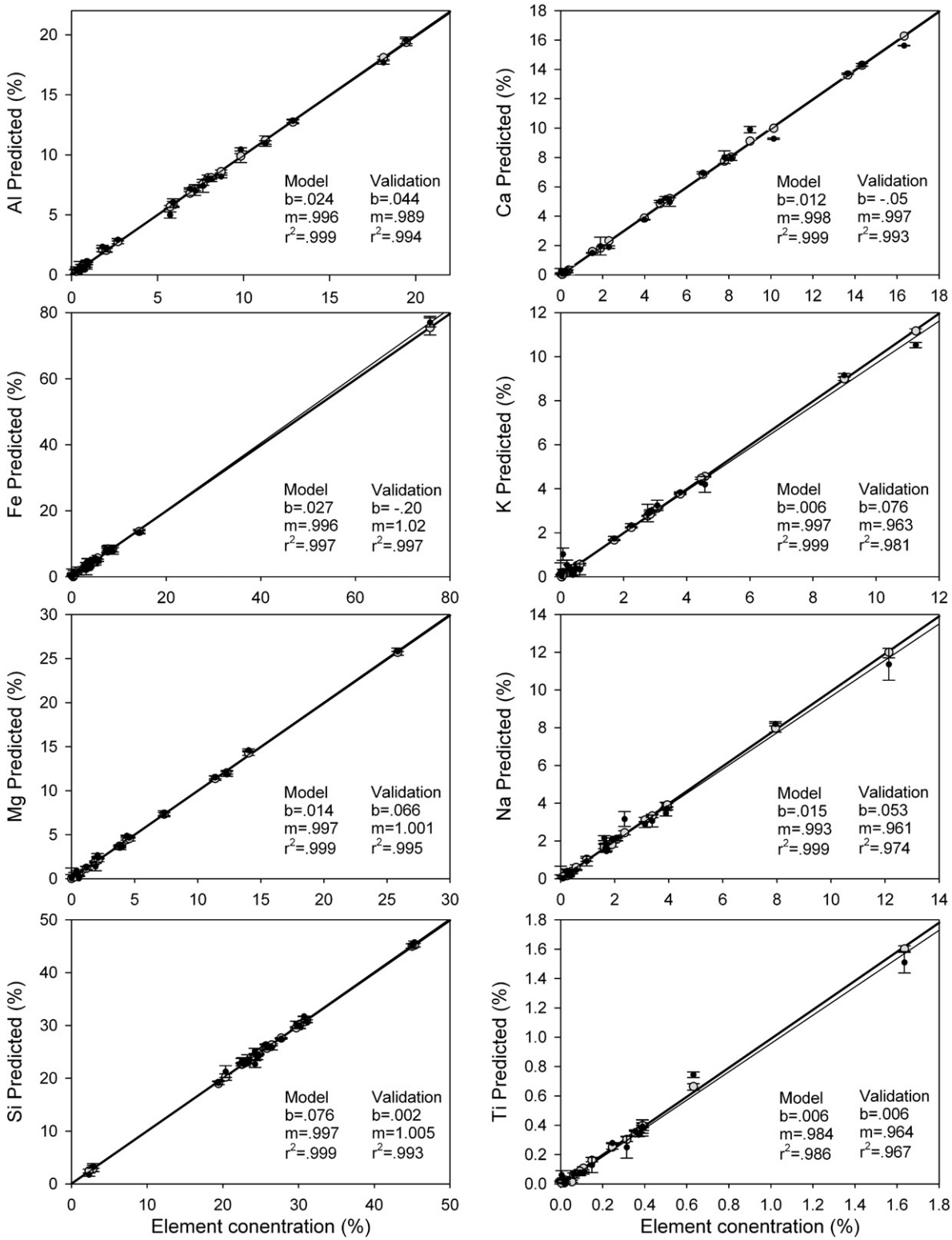

Fig. 4. Partial least squares regression models for eight major elements from 22 rock and mineral samples prepared as fused glass. Gray circles and the thick line represent the PLS model. Black circles and the thin line represent a separate validation dataset. Error bars are standard deviation of the spot-to-spot variations.

3.6. Partial least squares regression

The final analysis carried out was partial least squares regression models for the fused glass samples. The simple two variable regression models represented in Figs. 2 and 3 are better representations of the data quality because they represent the direct linear response of the analysis to element concentration. However, it is widely recognized that PLS models can compensate for some shortcomings in the LIBS results by simultaneously incorporating a large amount of data including all possible lines for a particular element as well as continuum data [18,31,37]. For the PLS models, 1916 lines commonly used for elements through atomic number 92 were extracted from the original spectra dataset (40,000 lines) and used to build the regression models. The list of common peaks was extracted from a database available through

the U.S. Army Research Laboratory. PLS models were developed for the eight major elements and for eight trace elements (Ba, Ce, Cr, Rb, Sr, V, Zn, Zr) which present additional challenges due to their low concentration. It has been argued that the entire spectral dataset can provide value to the regression as the PLS retains only the latent vectors that explain variance [38]. For this study the results of using all 40,000 data lines were compared to the results of using only the 1916 subset of common element peaks that were extracted from the datasets. The results were not dramatically different, but in almost all cases and truncated dataset yielded better results and are thus reported here. The PLS models for major elements were built using all 220 original shots (10 locations on 22 samples) with mean-center preprocessing. Data transforms included spectrum normalization to mitigate variations in plasma intensity and a Log10 transform which emphasizes small data

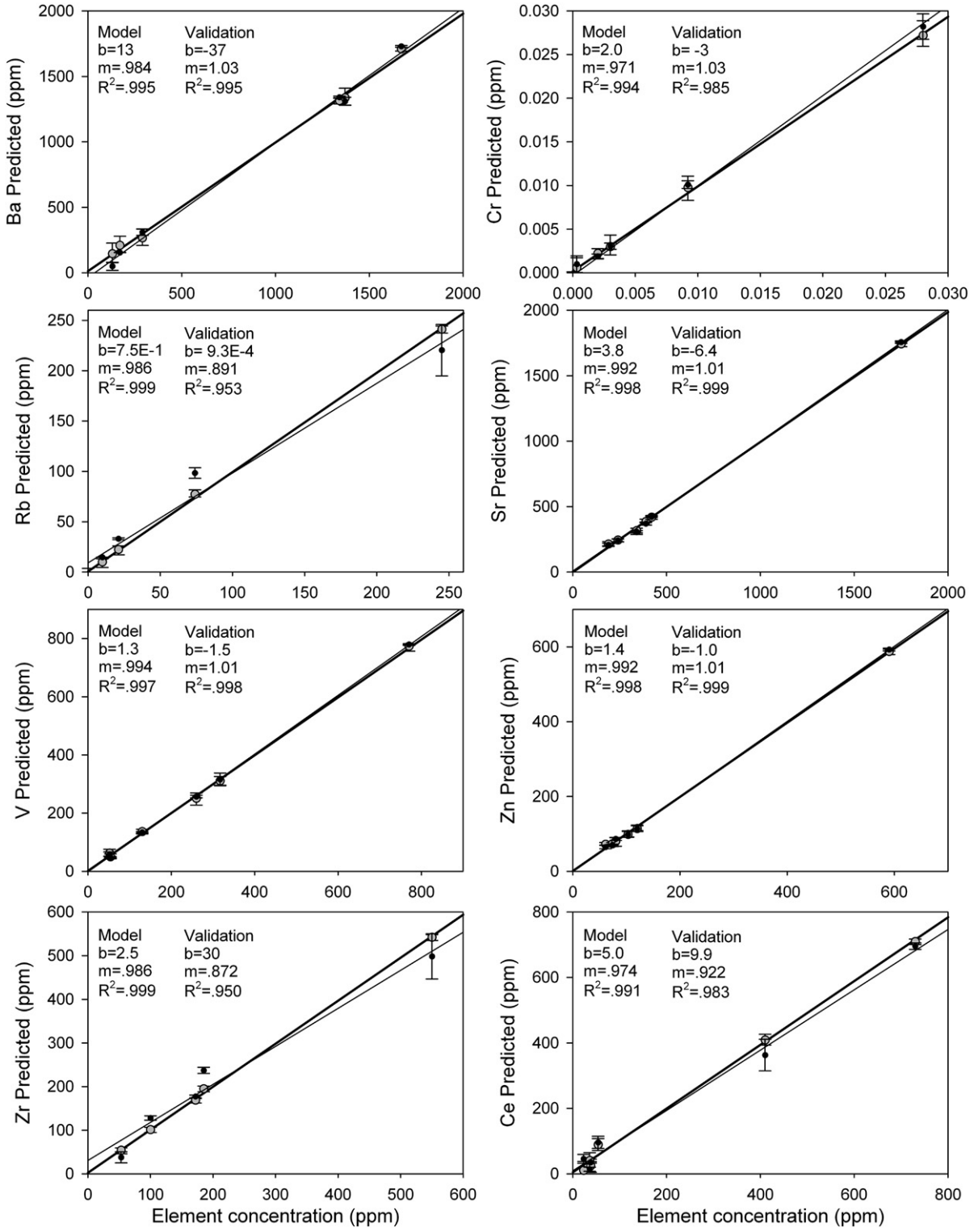

Fig. 5. Partial least squares regression models for eight minor elements from 22 rock and mineral samples prepared as fused glass. Gray circles and the thick line represent the PLS model. Black circles and the thin line represent a separate validation dataset. Error bars are standard deviation of the spot-to-spot variations.

values while deemphasizing larger ones and helps compensate for issues of heteroscedasticity [39]. This is important since the peak values do not have a linear relationship to absolute concentration across the entire spectrum and some elements, such as Ca, always produce large peaks relative to its actual concentration when compared to other elements. A second dataset of five analyses on the same samples were then predicted using the PLS model and plotted in Figs. 4 and 5. Trace element concentrations were known only for the six rock standards and thus those models were built using 60 shorts.

The results of the PLS models are very good showing R^2 values in the validation results above 0.96 for all eight major elements and above 0.95 for all trace elements (Figs. 4 and 5). Figs. 4 and 5 show both the original model and the validation results for each element which, in most cases, are almost identical. Among the major elements even Fe and Si, which were problematic in the single variable regression models, yielded excellent results. Only Na and Ti among the major elements, and Rb and Zr among the minor elements, showed high standard deviations in the validation data in high concentration samples. Despite minor issues, it is clear that the fused glass preparation can yield excellent PLS regression models. Results shown here were improved over some chemometric models presented in the literature for loose and pelletized powder samples [11,25] and were comparable to pelletized samples analyzed in a low-pressure, CO_2 environment [18] suggesting that the fused glass preparation can also provide enhanced results for multivariate models.

4. Conclusions

LIBS suffers from a matrix effect which can limit its ability to produce quantitative results in complex geologic materials. This study has shown that fused glass is a better method for developing samples/standards when conducting bulk analysis of rocks or minerals. This approach produces better results than does the more commonly used method of pressed powder pellets. The ANOVA results demonstrate that glass produces stronger separability between different sample materials across the eight major elements examined in this study and the coefficient of variation results showed improved precision for fused glass over pressed pellets. Likewise, simple regression models showed substantially better correlations and predictive ability in the glass than did those for the pressed pellets. Among the fused glass samples, Si was the only element that could not be modeled. Partial least squares regression provided an even better method of calibration and the results of those models for glass disks demonstrated excellent predictive ability for both major and trace elements. Low concentration values remained viable in the fused glass samples despite the 80% dilution of the sample with flux and extended to the trace elements in the PLS models.

The disadvantages of using fused glass preparations for LIBS bulk analysis is that it eliminates some of the advantages of LIBS, mainly the ability to forgo sample preparation. The preparation is not much more time consuming than preparing pressed pellets, but it does require specialized equipment with a much higher operational cost. Even though this preparation removes some of the advantages of LIBS regarding sample preparation, the glass material does provide a standardized preparation and instrument setup method so that calibration models could be extended to samples from many different sources without concern for matrix issues.

References

[1] R. Sattman, V. Sturm, R. Noll, Laser-induced breakdown spectroscopy of steel samples using multiple Q-switch Nd:YAG laser, J. Phys. D 28 (1995) 2181–2187.
[2] R. Sattman, I. Mönch, H. Krause, R. Noll, S. Couris, A. Hatziapostolou, C. Mavromanolakis, C. Fotakis, E. Larrauri, R. Miguel, Laser-induced breakdown spectroscopy for polymer identification, Appl. Spectrosc. 52 (1998) 456–461.
[3] H. Zhang, R.-Y. Yueh, J. Singh, Laser-induced breakdown spectrometry as a multimetal continuous-emission monitor, Appl. Opt. 38 (1999) 1459–1466.
[4] J. Gruber, J. Heitz, H. Strasser, D. Bauerle, N. Ramaseder, Rapid in-situ analysis of liquid steel by laser-induced breakdown spectroscopy, Spectrochim. Acta Part B 56 (2001) 685–693.
[5] R. Noll, H. Bette, A. Brysch, M. Kraushaar, I. Mönch, L. Peter, V. Strum, Laser-induced breakdown spectrometry — applications for production control and quality assurance in the steel industry, Spectrochim. Acta Part B 56 (2001) 637–649.
[6] L. St-Onge, J.-F. Archambault, E. Kwong, M. Sabsabi, E. Vadas, Rapid quantitative analysis of magnesium stearate in tablets using laser-induced breakdown spectroscopy, J. Pharm. Pharmaceut. Sci. 8 (2005) 272–288.
[7] B. Sallé, J.-L. Lacour, P. Mauchien, P. Fichet, S. Maurice, G. Manhès, Comparative study of different methodologies for quantitative rock analysis by laser-induced breakdown spectroscopy in a simulated Martian atmosphere, Spectrochim. Acta Part B 61 (2006) 301–313.
[8] J.-B. Sirven, B. Bousquet, L. Caniioni, L. Sarger, S. Tellier, M. Potin-Gautier, I. Le Hecho, Qualitative and quantitative investigation of chromium-polluted soils by laser-induced breakdown spectroscopy combined with neural networks analysis, Anal. Bioanal. Chem. 385 (2006) 256–262.
[9] J.-B. Sirven, B. Sallé, P. Mauchien, J.-L. Lacour, S. Maurice, G. Manhès, Feasibility study of rock identification at the surface of Mars by remote laser-induced breakdown spectroscopy and three chemometric methods, J. Anal. At. Spectrom. 22 (2007) 1471–1480.
[10] N. McMillan, R. Harmon, F. De Lucia, A. Miziolek, Laser-induced breakdown spectroscopy analysis of minerals: carbonates and silicates, Spectrochim. Acta Part B 62 (2007) 1528–1536.
[11] D. Death, A. Cunningham, L. Pollard, Multi-element and mineralogical analysis of mineral ores using laser induced breakdown spectroscopy and chemometric analysis, Spectrochim. Acta Part B 64 (2009) 1048–1058.
[12] J. Gottfried, F. De Lucia, C. Munson, A. Miziolek, Strategies for residue explosives detection using laser-induced breakdown spectroscopy, J. Anal. At. Spectrom. 23 (2008) 205–216.
[13] S. Pandhija, N. Rai, A. Rai, S. Thakur, Contaminant concentration in environmental samples using LIBS and CF-LIBS, Appl. Phys. B 98 (2010) 231–241.
[14] O. Samek, D.C.S. Beddows, H.H. Telle, G.W. Morris, M. Liska, J. Kaiser, Quantitative analysis of trace metal accumulation in teeth using laser-induced breakdown spectroscopy, Appl. Phys. A 69 (1999) S179–S182.
[15] V. Lazic, F. Colao, R. Fantoni, A. Paluccia, V. Spizzichinoa, I. Borgia, B.G. Brunetti, A. Sgamellotti, Characterisation of lustre and pigment composition in ancient pottery by laser induced fluorescence and breakdown spectroscopy, Anal. At. Spectrom. 19 (2004) 429–436.
[16] E. Rodreguez-Celis, I. Gornushkin, U. Heitmann, J. Almirall, B. Smith, J. Winefordner, N. Omenetto, Laser induced breakdown spectroscopy as a tool for discrimination of glass for forensic applications, Anal. Bioanal. Chem. 391 (2008) 1961–1968.
[17] B. Bousquet, J.-B. Sirven, L. Canioni, Spectrochim. Acta Part B 62 (2007) 1582–1589.
[18] S. Clegg, E. Sklute, M. Darby Dyar, J. Barefield, R. Wiens, Multivariate analysis of remote laser-induced breakdown spectroscopy spectra using partial least squares, principal component analysis, and related techniques, Spectrochim. Acta Part B 64 (2009) 79–88.
[19] L. Sun, H. Yu, Correction of self-absorption effect in calibration-free laser-induced breakdown spectroscopy by an internal reference method, Talanta 79 (2009) 388–395.
[20] E. Tognoni, G. Cristoforetti, S. Legnaioli, V. Palleschi, Calibration-free laser-induced breakdown spectroscopy: state of the art, Spectrochim. Acta Part B 65 (2010) 1–14.
[21] J. Anzano, M. Villoria, A. Ruíz-Medina, R. Lasheras, Laser-induced breakdown spectroscopy for quantitative spectrochemical analysis of geological materials: effects of the matrix and simultaneous determination, Anal. Chim. Acta 575 (2006) 230–235.
[22] C. Davies, H. Telle, A. Williams, Remote in situ analytical spectroscopy and its applications in the nuclear industry, Fresenius J. Anal. Chem. 355 (1996) 895–899.
[23] W.T.Y. Mohamed, Calibration free laser-induced breakdown spectroscopy (LIBS) identification of seawater salinity, Opt. Appl. 37 (2007) 5–19.
[24] N. McMillan, C. McManus, R. Harmon, F. De Lucia, A. Miziolek, Laser-induced breakdown spectroscopy analysis of complex silicate minerals — beryl, Anal. Bioanal. Chem. 385 (2006) 263–271.
[25] J. Tucker, M. Dyar, M. Schaefer, S. Clegg, R. Wiens, Optimization of laser-induced breakdown spectroscopy for rapid geochemical analysis, Chem. Geol. 277 (2010) 137–148.
[26] P. Yaroshchyk, D. Body, R. Morrison, B. Chadwick, A semi-quantitative standard-less analysis method for laser-induced breakdown spectroscopy, Spectrochim. Acta Part B 61 (2006) 200–209.
[27] E. Tognoni, G. Cristoforetti, S. Legnaioli, V. Palleschi, A. Salvetti, M. Mueller, U. Panne, I. Gornushkin, A numerical study of expected accuracy and precision in calibration-free laser-induced breakdown spectroscopy in the assumption of ideal analytical plasma, Spectrochim. Acta Part B 62 (2007) 1287–1302.
[28] D. Díaz Pace, N. Gabriele, M. Garcimuño, C. D'Angelo, G. Bertuccelli, D. Bertuccelli, Analysis of minerals and rocks by laser-induced breakdown spectroscopy, Specto. Lett. 44 (2011) 399–411.
[29] B. Lal, L. St-Onge, F.-Y. Yueh, J. Singh, in: J. Singh, S. Thakur (Eds.), Laser-induced Breakdown Spectroscopy, Elsevier, Amsterdam, 2007, pp. 287–310.
[30] V. Lazic, R. Rantoni, F. Colao, A. Santagata, A. Morone, V. Spizzichino, Quantitative laser induced breakdown spectroscopy analysis of ancient marbles and corrections for the variability of plasma parameters and of ablation rate, J. Anal. At. Spectrom. 19 (2004) 429–436.
[31] S. Laville, M. Sabsabi, F. Doucet, Multi-elemental analysis of solidified mineral melt samples by laser-induced breakdown spectroscopy coupled with a linear multivariate calibration, Spectrochim. Acta Part B 62 (2007) 1557–1566.
[32] J. Carranza, D. Hahn, Sampling statistics and considerations for single-shot analysis using laser-induced breakdown spectroscopy, Spectrochim. Acta Part B 57 (2002) 779–790.

[33] S. Buckley, Laser-induced breakdown spectroscopy for toxic metal emission measurements: experimental considerations and oxygen quenching, Environ. Eng. Sci. 22 (2005) 195–204.
[34] D. Cremers, L. Radziemski, Handbook of laser-induced breakdown spectroscopy, Wiley, West Sussex, 2006.
[35] B. Thompson, N. McMillan, Effect of bond strength on Al and Si ablation and intensity in laser-induced breakdown spectroscopy (LIBS), Geologic Society of America Meeting 2008, Paper 156-9, 2008.
[36] W.T. Mohamed, Improved LIBS limit of detection of Be, Mg, Si, Mn, Fe and Cu in aluminum alloy samples using a portable Echelle spectrometer with ICCD camera, Opt. Laser Technol. 40 (2008) 30–38.
[37] J. Gottfried, R. Harmon, F. De Lucia, A. Miziolek, Multivariate analysis of laser-induced breakdown spectroscopy chemical signatures for geomaterial classification, Spectrochim. Acta Part B 64 (2009) 1009–1019.
[38] H. Abdi, Encyclopedia of Measurement and Statistics, in: N. Salkind (Ed.), Sage, Thousand Oaks, 2007, pp. 1–13.
[39] H. Idborg, P.-O. Edlund, S. Jacobsson, Multivariate approaches for efficient detection of potential metabolites from liquid chromatography/mass spectrometry data, Rapid Commun. Mass Spectrom. 18 (2004) 944–954.
[40] R. Colao, R. Fantoni, V. Lazic, A. Paolini, F. Rabbri, G. Ori, L. Marinangeli, A. Baliva, Investigation of LIBS feasibility for in situ planetary exploration: an analysis on Martian rock analogues, Planet. Space Sci. 52 (2004) 117–123.
[41] L. St-Onge, M. Sabsabi, Towards quantitative depth-profile analysis using laser-induced plasma spectroscopy: investigation of galvannealed coatings on steel, Spectrochim. Acta Part B 55 (2000) 299–308.
[42] J. Vadillo, C. Garcia, S. Palanco, J. Laserna, Nanometric range depth-resolved analysis of coated-steels using laser-induced breakdown spectrometry with a 308 nm collimated beam, J. Anal. At. Spectrom. 13 (1998) 793–797.